

## Interpretation of the $(d, \alpha)$ Reactions on $F^{19}$ and $N^{15}$ at 20.9 MeV

JOSEPH R. PRIEST\* AND JOHN S. VINCENT

*Lewis Research Center, National Aeronautics and Space Administration, Cleveland, Ohio*

(Received 16 August 1967)

The differential cross sections corresponding to the production of the first three and first two residual states in the reactions  $F^{19}(d, \alpha)O^{17}$  and  $N^{15}(d, \alpha)C^{13}$  have been measured from  $17^\circ$  to  $170^\circ$  and  $17^\circ$  to  $112^\circ$ , respectively, for a deuteron energy of 20.9 MeV (lab). The shapes of the angular distributions are consistent with a cutoff-radius distorted-wave Born-approximation calculation using the zero-range approximation for the nuclear interaction. The best fit was obtained for the  $F^{19}(d, \alpha)O^{17}$  which proceeded primarily by  $L=0$  orbital-angular-momentum transfer. Arguments based on the character of the nuclear states involved and the magnitudes of the experimental differential cross sections indicate that the most favorable reaction mechanism is the pickup of a neutron-proton pair from the target nucleus.

### INTRODUCTION

THE reaction  $F^{19}(d, \alpha)O^{17}$  leading to the ground and low-lying states of  $O^{17}$  has been investigated for several energies between 5.5 and 14.7 MeV.<sup>1-4</sup> In general, the angular distributions exhibit an oscillatory-type structure, with some large angle peaking which tends to decrease as the deuteron energy increases. These data have been analyzed primarily by assuming a two-nucleon pickup mechanism and using either a plane-wave (PWBA)<sup>5-11</sup> or distorted-wave Born-approximation (DWBA)<sup>12-14</sup> calculation. The DWBA pickup calculation is appropriate for reactions in which the final state can be formed by the simple extraction of a neutron-proton pair from the target nucleus. The recent analysis of Wesolowski *et al.*,<sup>4</sup> using shell-model configurations for  $F^{19}$  and the ground state of  $O^{17}$ , has demonstrated the applicability of the DWBA pickup calculation for deuteron energies of 10.2 and 11.5 MeV. It is interesting that the cross sections for production of some of the states of  $O^{17}$ , which are not readily formed by the simple removal of a neutron-proton pair from  $F^{19}$ , are comparable to those corresponding to production of the characteristic shell-model states. In addition, the angular distributions display many of the characteristics of a pickup process. However, the energy dependence of the differential and integrated cross sections indicates that the reaction mechanism may simplify for higher deuteron energies. The present investigation of

the  $F^{19}(d, \alpha)O^{17}$  reaction at 20.9 MeV was carried out with the hope of clarifying the reaction mechanism.

In order to gain additional insight into the  $(d, \alpha)$  reaction mechanism, the  $N^{15}(d, \alpha)C^{13}$  reaction leading to the ground and first excited states of  $C^{13}$  was also studied. Although this reaction was studied previously by Fischer and Fischer<sup>15</sup> at essentially the same deuteron energy, only the ground state of  $C^{13}$  was resolved.

### PROCEDURE

The Lewis Research Center fixed-energy cyclotron provided a source of  $21.0 \pm 0.1$ -MeV deuterons. The particle-detection and discrimination scheme was the same as that used in a previous  $(d, \alpha)$  experiment.<sup>16</sup> The  $F^{19}$  targets used were  $1.43 \pm 0.05$ -mg/cm<sup>2</sup> commercial films of Teflon<sup>17</sup> ( $CF_2$ ). Alpha particles of interest from the  $F^{19}(d, \alpha)O^{17}$  reaction were distinguished from those from the  $C^{12}(d, \alpha)B^{10}$  reaction by virtue of the large difference in  $Q$  values ( $+10.038$  and  $-1.351$  MeV, respectively). As anticipated, the Teflon targets deteriorated as a result of the deuteron bombardment, even though the beam current was about 30 nA. Consequently, each target was changed after  $15 \mu C$  of charge had accumulated in the Faraday cup. A fixed-angle counter, which recorded deuterons scattered elastically from  $C^{12}$  and  $F^{19}$ , monitored the target thickness. The internal consistency of the data justifies this procedure.

$N^{15}$  gas having a purity of 99%<sup>18</sup> was used for the  $N^{15}(d, \alpha)C^{13}$  experiment. It was contained in a cylindrical gas cell  $4\frac{3}{4}$  in. in diam and  $\frac{3}{4}$  in. thick. The walls of the cell were covered with Havar foil<sup>19</sup> 0.0001 in. thick. The pressure was measured with a resistance-type strain-gauge transducer to an accuracy of 0.05 mm Hg. The nominal pressure of the gas was 14.5 mm Hg. The ambient temperature of the gas was measured to an accuracy of 0.5°K with an iron-constantan thermo-

\* Permanent address: Physics Department, Miami University, Oxford, Ohio.

<sup>1</sup> C. Hu, J. Phys. Soc. Japan **15**, 1741 (1960).

<sup>2</sup> K. Takamatsu, J. Phys. Soc. Japan **17**, 896 (1962).

<sup>3</sup> S. W. Cospser, B. T. Lucas, and O. E. Johnson, Phys. Rev. **138**, B51 (1965).

<sup>4</sup> J. J. Wesolowski, L. F. Hansen, J. G. Vidal, and M. L. Stelts, Phys. Rev. **148**, 1063 (1966).

<sup>5</sup> H. C. Newns, Proc. Phys. Soc. (London) **A76**, 489 (1960).

<sup>6</sup> M. El Nadi, Proc. Phys. Soc. (London) **A70**, 62 (1957).

<sup>7</sup> M. El Nadi and M. El Khishin, Proc. Phys. Soc. (London) **A73**, 705 (1959).

<sup>8</sup> M. El Nadi, Phys. Rev. **119**, 242 (1960).

<sup>9</sup> S. T. Butler and O. H. Hittmair, *Nuclear Stripping Reactions* (John Wiley & Sons, Inc., New York, 1957).

<sup>10</sup> M. L. Rustgi, Nucl. Phys. **25**, 169 (1961).

<sup>11</sup> I. Manning and A. H. Aitken, Nucl. Phys. **32**, 524 (1962).

<sup>12</sup> W. Tobocman, *Theory of Direct Nuclear Reactions* (Oxford University Press, London, 1961).

<sup>13</sup> N. K. Glendenning, Ann. Rev. Nucl. Sci. **13**, 191 (1963).

<sup>14</sup> N. K. Glendenning, Phys. Rev. **137**, B102 (1965).

<sup>15</sup> G. E. Fischer and V. K. Fischer, Phys. Rev. **114**, 533 (1959).

<sup>16</sup> J. R. Priest and J. S. Vincent, Phys. Rev. **152**, 989 (1966).

<sup>17</sup> These films were manufactured by the Dilectrix Corp., Farmingham, Long Island, N. Y., and were kindly donated by Professor O. E. Johnson, Purdue University.

<sup>18</sup> Obtained from Isomet Corp., 433 Commercial Ave., Palisades Park, N. J.

<sup>19</sup> Havar is a cobalt-base high-strength alloy manufactured by the Hamilton Watch Co., Lancaster, Pa.

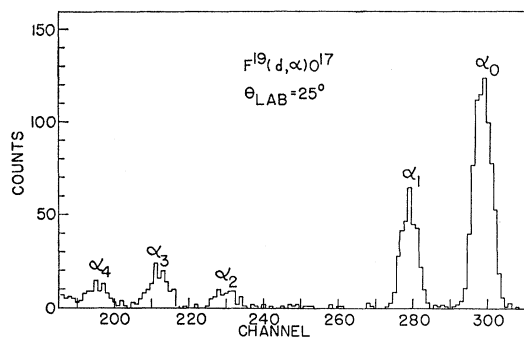


FIG. 1. Typical  $\alpha$ -particle spectrum for the reaction  $F^{19}(d, \alpha)O^{17}$  at a laboratory reaction angle of  $25^\circ$ .

couple, using an ice-water mixture as a reference temperature.

### EXPERIMENTAL RESULTS

The over-all energy resolution was about 300 keV full width at half-maximum (FWHM). This was adequate to completely resolve the ground and first two excited states of  $O^{17}$  and the ground and first excited state of  $C^{13}$  (Figs. 1 and 2). The third and fourth excited states of  $O^{17}$  were partially resolved, which permitted a reasonable estimate of the differential cross sections for production of these states. These were subsequently used to extract integrated cross sections. The angular distributions are shown in Figs. 3-8. The experimental data are tabulated elsewhere.<sup>20</sup> The quoted errors are due only to statistical uncertainties. The probable systematic error in the absolute differential cross section is estimated to be 15%.

### DISCUSSION

The common characteristics of the data are the following: (1) All of the angular distributions have some semblance to that expected for a simple direct-interaction process. They are all peaked in the forward direc-

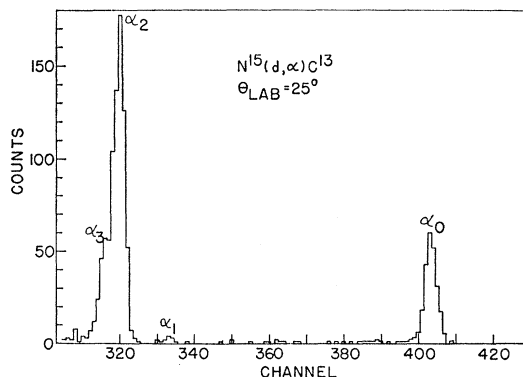


FIG. 2. Typical  $\alpha$ -particle spectrum for the reaction  $N^{15}(d, \alpha)C^{13}$  at a laboratory reaction angle of  $25^\circ$ .

<sup>20</sup> J. R. Priest and J. S. Vincent, NASA Tech. Note D-3813 (unpublished).

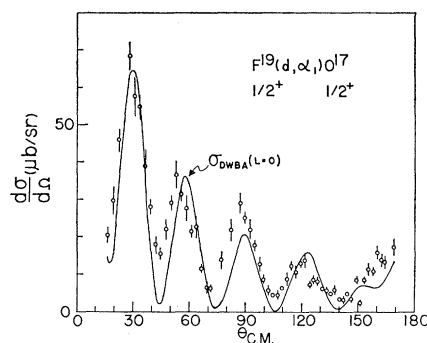


FIG. 3. Angular distribution of differential cross sections for  $F^{19}(d, \alpha)O^{17}$ , leaving  $O^{17}$  in the first excited state. The curve represents a cutoff-radius DWBA calculation for  $L=0$ .

tion, and there is little enhancement of the differential cross sections at large angles. (2) The most distinct direct-reaction-type pattern is seen in the angular distributions corresponding to the production of the 0.871-MeV first excited state of  $O^{17}$  and the ground state of  $C^{13}$ . The angular distributions suggest that the reaction mechanism is simple and that an interpretation may be possible within the framework of a direct-reaction model. (3) The differential cross sections for production of the 3.058-MeV second excited state of  $O^{17}$  and the 3.09-MeV first excited state of  $C^{13}$  are noticeably smaller than those for the other states of the same residual nucleus.

Some additional insight into the reaction mechanism is obtained from the integrated cross sections. The present data were integrated from  $20^\circ$  to  $170^\circ$ , and are shown, along with all other available data, in Fig. 9. There is some structure at lower energies where compound-nucleus effects are expected to be important. However, for energies greater than about 11 MeV, the structure is small, and all cross sections decrease approximately monotonically as the energy increases. The behavior is very much the same for all five states of  $O^{17}$ . This linear relationship between  $\ln \sigma$  and  $E_d$  is characteristic of a direct reaction, and can be understood, for example, in terms of the plane-wave formalism of

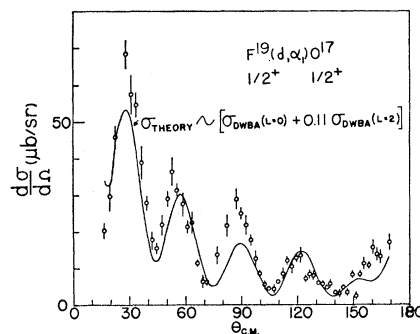


FIG. 4. Angular distribution of differential cross sections for  $F^{19}(d, \alpha)O^{17}$ , leaving  $O^{17}$  in the first excited state. The curve represents an incoherent mixture of the  $L=0$  and  $L=2$  cutoff-radius DWBA calculations.

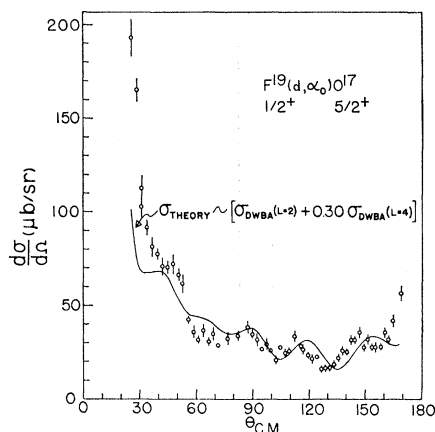


FIG. 5. Angular distribution of differential cross sections for  $F^{19}(d, \alpha)O^{17}$ , leaving  $O^{17}$  in the ground state. The curve represents an incoherent mixture of the  $L=2$  and  $L=4$  cutoff-radius DWBA calculations.

Newns.<sup>21</sup> For a reaction of the form  $X(d, \alpha)Y$ , Newns expresses the differential cross section for the pickup of a neutron-proton pair from the target nucleus as

$$\frac{d\sigma}{d\Omega} \sim e^{-(k^2/8\gamma^2)} \sum_L A_L^2 j_L^2(Qr), \quad (1)$$

where

$$K^2 = \mathbf{K} \cdot \mathbf{K} = \frac{1}{4}k_\alpha^2 + k_d^2 - k_\alpha k_d \cos\theta,$$

$$\mathbf{Q} = \mathbf{k}_\alpha - (M_Y/M_X)\mathbf{k}_d,$$

$\mathbf{k}_\alpha$  and  $\mathbf{k}_d$  are the c.m. wave vectors associated with the  $\alpha$  particle and deuteron,  $\gamma$  is the parameter associated with the Gaussian form of the  $\alpha$ -particle wave function  $\psi_\alpha = N \exp(-\gamma^2 \sum_{i<j} r_{ij}^2)$ ,  $L\hbar$  is the orbital angular momentum transferred,  $j_L$  is a spherical Bessel function, and  $A_L$  is the structure factor. Since  $K$  and  $Q$  depend on the deuteron energy, the integrated cross section will depend on energy through both the exponential term and  $j_L$ . However, the main dependence is in the exponential term. Assuming that the energy dependence is contained only in the exponential term the integrated cross section can be written as  $d\sigma/d\Omega \sim e^{-\beta E_d/8\gamma^2}$ , where

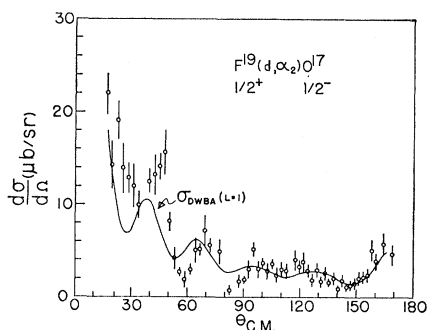


FIG. 6. Angular distribution of differential cross sections for  $F^{19}(d, \alpha)O^{17}$ , leaving  $O^{17}$  in the second excited state. The curve represents a cutoff-radius DWBA calculation for  $L=1$ .

<sup>21</sup> H. C. Newns, Proc. Phys. Soc. (London) **76**, 489 (1960).

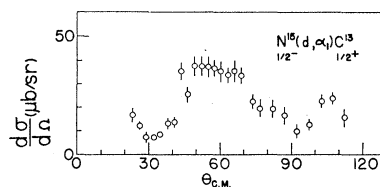


FIG. 7. Angular distribution of differential cross sections for  $N^{16}(d, \alpha)C^{13}$ , leaving  $C^{13}$  in the first excited state.

$\beta$  is a constant which arises in the calculation of  $k_\alpha^2$  and  $k_d^2$ . The observed linear relationship (Fig. 9) between  $\ln\sigma$  and  $E_d$  then follows from this expression. Fitting this expression to the ground-state data for  $E_d \geq 11.5$  MeV yields a value of  $0.34 F^{-1}$  for  $\gamma$ . This value is within 10% of that used by experimenters<sup>2,22-24</sup> who used Newns theory (or variations thereof) for fitting angular-distribution data.

This similar behavior of the integrated cross sections versus energy for all five states of  $O^{17}$  is interesting because the character of these states is quite different. The ground and first excited states of  $O^{17}$  (Fig. 10)<sup>25</sup> may be readily interpreted, assuming that  $O^{17}$  is an inert  $O^{16}$  core plus a neutron in a  $1d_{5/2}$  orbital for the ground state and in a  $2s_{1/2}$  orbital for the first excited state.<sup>26</sup> The study of the  $O^{16}(d, p)O^{17}$  stripping reaction confirms

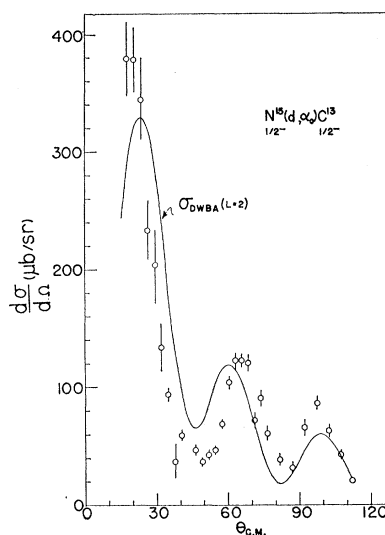


FIG. 8. Angular distribution of differential cross sections for  $N^{16}(d, \alpha)C^{13}$ , leaving  $C^{13}$  in the ground state. The curve represents a cutoff-radius DWBA calculation for  $L=2$ .

<sup>22</sup> T. Yanabu, S. Yamashita, T. Nakamura, K. Takamatsu, A. Msaiké, S. Kakigi, Dai Ca Nguyen, and K. Takimoto, J. Phys. Soc. Japan **17**, 914 (1962).

<sup>23</sup> S. W. Cosper, B. T. Lucas, and O. E. Johnson, Phys. Rev. **138**, B610, (1965).

<sup>24</sup> S. W. Cosper, B. T. Lucas, and O. E. Johnson, Phys. Rev. **139**, B763 (1965).

<sup>25</sup> F. Ajzenberg-Selove and T. Lauritsen, Nucl. Phys. **11**, 1 (1959).

<sup>26</sup> M. A. Preston, *Physics of the Nucleus* (Addison-Wesley Publishing Co., Inc., Reading, Mass., 1962), p. 184.

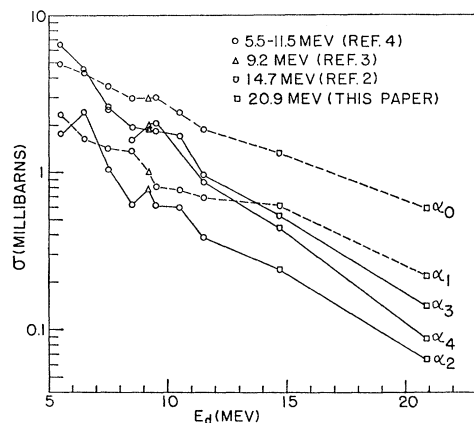


FIG. 9. The  $F^{19}(d,\alpha)O^{17}$  differential cross sections integrated from  $20^\circ$  to  $170^\circ$  plotted against the deuteron energy in the laboratory system.

these assignments.<sup>27</sup> In the same study, the differential cross sections for production of the 3.058-MeV state are very small and the angular distribution is isotropic within experimental uncertainties. The formation of this state is assumed to require excitation of a nucleon from the  $O^{16}$  core. The angular distributions corresponding to production of the 3.846- and 4.555-MeV states exhibit weak  $l_n=2$  and  $1_n=1$  stripping-type patterns, respectively. The assignment of spin and parity  $\frac{3}{2}^-$  to the 3.846-MeV state would be consistent with the capture of a neutron into a single-particle  $1f_{7/2}$  orbital. However, more recent measurements indicate that the spin and parity of this state are  $\frac{5}{2}^-$ ,<sup>3,28,29</sup> and that this state and the one at 4.555 MeV require excitation of a nucleon from the  $O^{16}$  core for its formation.<sup>30</sup> The production of these

5.08	$3/2^+$
4.555	$3/2^-$
3.846	$5/2^-$
3.058	$1/2^-$
0.871	$1/2^+$
GND.	$5/2^+$

$O^{17}$

FIG. 10. Low-lying levels of  $O^{17}$ . The energies are taken from Ref. 25. The spin and parity assignments are discussed in the text.

<sup>27</sup> T. S. Green and R. Middleton, Proc. Phys. Soc. (London) **A69**, 28 (1956).

<sup>28</sup> R. E. Segal, P. P. Singh, R. G. Allas, and S. S. Hanna, Phys. Rev. Letters **10**, 345 (1963).

<sup>29</sup> C. Broude, T. K. Alexander, and A. E. Litherland, Bull. Am. Phys. Soc. **8**, 26 (1963).

<sup>30</sup> J. P. Elliott and B. H. Flowers, Proc. Phys. Soc. (London) **A229**, 536 (1955).

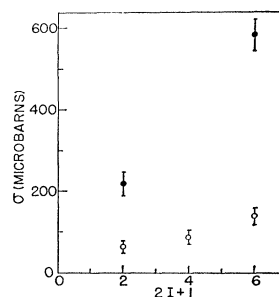


FIG. 11. The  $F^{19}(d,\alpha)O^{17}$  differential cross sections integrated from  $20^\circ$  to  $170^\circ$  plotted against  $2I+1$ , where  $I$  is the spin quantum number of the residual state. The solid circles represent the ground and first excited states of  $O^{17}$ . The open circles represent the second, third, and fourth core-excited states of  $O^{17}$ .

states in any direct  $(d,\alpha)$  process would be a second-order effect, and this seems to be borne out by the significantly smaller integrated cross sections for  $E_d \geq 14.7$  MeV. The shape of the integrated cross-section-versus-energy curve is also indicative of a direct-reaction process.

In several  $(d,\alpha)$  reactions at low energies, it has been found that the integrated cross sections are proportional to  $2I+1$ .<sup>28,31-33</sup> It is clear from Fig. 9 that there is little, if any, validity of this rule for the  $F^{19}(d,\alpha)O^{17}$  reaction, even at the lower energies. Nevertheless, an interesting correlation is observed in the integrated cross-sections-versus- $2I+1$  plot in Fig. 11. The two solid points correspond to the well-defined single-particle states, while the open circles correspond to the excited-core states of  $O^{17}$ . An approximate proportionality between the integrated cross sections for production of a given type of state and  $2I+1$  is observed. The data at 14.7 MeV also exhibit the same behavior.<sup>2</sup>

#### ANALYSIS OF EXPERIMENTAL DATA

The previous discussion of the gross character of the angular distributions and integrated cross sections indicates that a more detailed direct-reaction analysis is appropriate. The DWBA theory as formulated by Tobocman<sup>12</sup> was chosen for this analysis. The cutoff-radius DWBA of a FORTRAN code written by Gibbs *et al.*<sup>34</sup> was used for the numerical calculations. This calculation employed the zero-range approximation for the nuclear interaction. There are two aspects of these calculations which should be discussed in some detail.

(1) In the cutoff-radius approach, all contributions to the transition amplitude are neglected for radial distances less than the cutoff radius. The physical rationale behind this approach is certainly questionable. Nevertheless, in many direct-reaction analyses, this technique has noticeably improved the agreement between theory and experiment.<sup>35</sup> In an effort to explain this and also

<sup>31</sup> S. Hinds, R. Middleton, and A. E. Litherland, in *Proceedings of the Rutherford Jubilee International Conference, Manchester, 1961* (Heywood and Co., Ltd., London, 1961), p. 305.

<sup>32</sup> N. MacDonald, Nucl. Phys. **33**, 110 (1962).

<sup>33</sup> O. Hansen, E. Koltay, N. Lund, and B. S. Madsen, Nucl. Phys. **51**, 307 (1964).

<sup>34</sup> W. R. Gibbs, V. A. Madsen, J. A. Miller, W. Tobocman, E. C. Cox, and L. Mowry, NASA Tech. Note D-2170 (1964) (unpublished).

<sup>35</sup> G. R. Satchler, Argonne National Laboratory Report No. ANL-6878, 1964, p. 29 (unpublished).

why DWBA calculations are sometimes inconsistent in explaining experimental results, Buck and Rook<sup>36</sup> have examined the DWBA formalism in general. Their conclusions can be briefly summarized as follows: (a) "It is very suspect to use the DWBA for reactions other than deuteron stripping or inelastic scattering to low-lying states, and even these may be suspect if the angular-momentum transfer  $L$  is large or the initial and final momenta are widely different," (b) in the cutoff-radius DWBA, ambiguities in the optical potentials used for fitting the elastic scattering results are irrelevant, and (c) the cutoff radius is to be treated as a phenomenological parameter, but should be about 1 F larger than the nuclear radius. The analysis of our data is to be considered a test of these ideas.

(2) A  $(d, \alpha)$  reaction is customarily viewed as either the pickup of a neutron-proton pair from the target nucleus or the direct knockout of an  $\alpha$  particle from the target nucleus. In a low-resolution survey of  $(d, \alpha)$  reactions using 15-MeV deuterons on nuclei from  $Z=28-83$ , Mead and Cohen<sup>37,38</sup> observed two strong peaks in the  $\alpha$ -particle-energy spectra. They concluded that the low-energy peak is in accord with statistical compound-nucleus theory and that the principal features of the high-energy peak can be explained on the basis of a two-nucleon pickup process. Furthermore, it has been concluded that  $(p, t)$ ,  $(p, He^3)$ , and  $(p, \alpha)$  reactions on  $O^{16}$ , which should be much like  $(d, \alpha)$  reactions on light nuclei, also proceed by a pickup process.<sup>39</sup> The pickup mechanism is certainly more appealing within the context of a shell-model description of the target and residual nuclei. The cutoff-radius DWBA calculation employed here determines the shape of the angular distribution, but not the absolute magnitude. Just as in simple plane-wave calculations, the reaction mechanism cannot be distinguished on the basis of the shape of the angular distribution.<sup>40</sup> Some effort is made, however, to differentiate between the processes on the basis of the shell-model description of the nuclei involved and the relative magnitudes of the experimental cross sections.

The elastic scattering wave functions for the incident and exit channels were generated using a Woods-Saxon potential of the form

$$V_c - (V + iW)/(1 + e^x), \quad x = (r - R)/a, \quad (2)$$

where  $V_c$  is the Coulomb potential for a uniformly charged sphere of radius  $R$ . Ideally, the parameters for the incident deuteron and exit  $\alpha$ -particle channels should be obtained from an optical-model fit to the elastic scattering data at the proper c.m. energies. There are, however, no such data available for this analysis. Our

experience in the optical-model analysis of 40-MeV  $\alpha$ -particle-scattering experiments on light nuclei has shown that reasonable fits can be obtained, at least up to  $90^\circ$ , using a set of parameters which do not vary appreciably from nucleus to nucleus.<sup>41</sup> There are, of course, ambiguities in sets of parameters. The parameters for the deuteron channel are somewhat more difficult to estimate. Realistically, the optical potential should contain a spin-orbit term. However, the direct-reaction code used did not include a spin-orbit term. An examination of the literature for optical-model analyses of deuteron elastic scattering using the above-mentioned simple Woods-Saxon form showed that reasonable fits could be obtained without having extreme variations in the parameters.<sup>42,43</sup> Therefore, a typical set was chosen. The cutoff-radius DWBA calculation, which should not be particularly sensitive to either ambiguities in the optical potential or details of the parameters, will justify this procedure. The parameters chosen for the  $F^{19}(d, \alpha)O^{17}$  analysis are shown in Table I. These parameters were fixed throughout the calculation. Only the cutoff-radius parameter was varied.

TABLE I. Optical-model parameters used in DWBA calculations. The radius of the uniformly charged sphere for the Coulomb potential was also equal to  $R$ .

	$V$ (MeV)	$W$ (MeV)	$a$ (F)	$R$ (F)
Deuteron channel	+55	+11	0.65	3.95
$\alpha$ -particle channel	33	9	0.50	4.54

In the DWBA calculation employed here, the bound-state wave functions for the exchanged particles (taken as a lump) were eigenfunctions of a Woods-Saxon Hamiltonian, with eigenenergy equal to the binding energy of the lump. The cutoff radii were 1-2 F larger than the radius of the Woods-Saxon potential having a diffuseness parameter of 0.4 F. Thus the DWBA form factor was essentially a monotonically decreasing exponential function of the radius  $r$ . The calculation of the shape of the angular distribution is therefore insensitive to the quantum parameters of the bound particles. This procedure negates any comparison of ratios of cross sections leading to different states of the residual nucleus.

### $F^{19}(d, \alpha_1)O^{17}$

We chose to analyze these data first because of the apparent simplicity in the angular-distribution pattern. This circumstance allowed us to determine the appropriate cutoff-radius parameter which was used in subsequent calculations. The selection rules for transitions to the first excited state of  $O^{17}$  allow  $L=0$  and 2, where  $L$

<sup>36</sup> B. Buck and J. R. Rook, Nucl. Phys. **67**, 504 (1965).

<sup>37</sup> J. B. Mead and B. L. Cohen, Phys. Rev. Letters **5**, 105 (1960).

<sup>38</sup> J. B. Mead and B. L. Cohen, Phys. Rev. **125**, 947 (1962).

<sup>39</sup> J. Cerny and R. H. Pehl, Argonne National Laboratory Report No. ANL-6878, 1964, p. 479 (unpublished).

<sup>40</sup> N. Austern, in *Selected Topics in Nuclear Theory*, edited by F. Janouch (International Atomic Energy Agency, Vienna, 1963), p. 30.

<sup>41</sup> J. R. Priest, J. S. Vincent, E. T. Boschitz, and R. W. Bercaw, in *Proceedings of the International Conference on Nuclear Physics, Paris, 1964* (Editions du Centre National de la Recherche Scientifique, Paris, 1965), Vol. II, p. 888.

<sup>42</sup> R. H. Pehl, J. Cerny, E. Rivet, and B. G. Harvey, Phys. Rev. **140**, B605 (1965).

<sup>43</sup> H. R. E. Tjin A. Djie, and K. W. Brockman, Jr., Nucl. Phys. **74**, 417 (1965).

is the orbital-angular-momentum transfer. However, the well-defined oscillatory pattern with deep minima is very characteristic of a pure  $L=0$  orbital-angular-momentum transfer.<sup>44</sup> The cutoff-radius DWBA calculation for  $L=0$  and a cutoff radius of 4.58 F is shown as the solid line in Fig. 3. The agreement with experiment is quite satisfactory over the entire angular range studied. The main deficiency is that the experimental minima are shallower than those predicted by theory. It is presumptuous, however, on the basis of the simplicity of the model employed, to expect exceptional agreement without at least including some contribution from the  $L=2$  DWBA calculation. While it is not uncommon to treat the nuclear-structure coefficients associated with the different allowed  $L$  components as adjustable parameters, the procedure is questionable.<sup>4</sup> Since the direct-reaction code employed here is equipped to handle only a single  $L$  value, some provision must be made to mix incoherently the components for the various values of  $L$ . Although we treat the structure factors as adjustable parameters, the arbitrariness of this choice is minimized by using the following procedure: Using exactly the same optical-model-potential parameters and cutoff radius as for the  $L=0$  calculation, we repeated the calculation for  $L=2$ . We then mixed the  $L=0$  and  $L=2$  calculations by determining the normalizing constants  $\beta$  and  $\gamma$  which minimized the  $\chi^2$  function defined by

$$\chi^2 = \sum_{\theta} \left( \frac{\beta\sigma_{L=0}(\theta) + \gamma\sigma_{L=2}(\theta) - \sigma_{\text{expt}}(\theta)}{\Delta\sigma_{\text{expt}}} \right)^2. \quad (3)$$

Here  $\sigma_L$  is the differential cross section obtained by DWBA,  $\sigma_{\text{expt}}$  is the experimental differential cross section, and  $\Delta\sigma_{\text{expt}}$  is the statistical uncertainty in the experimental cross section. The result of adding 11% of the  $L=2$  component is shown in Fig. 4. The agreement with experiment is not exceptionally better than that obtained using only the  $L=0$  contribution (Fig. 3), but it is more realistic in the sense that there is much better agreement at the minima.

With regard to the ideas of Buck and Rook<sup>36</sup> concerning the cutoff DWBA, we note that the cutoff radius used, 4.58 F, is indeed about 1 F greater than the nuclear radius of  $F^{19}$  if we assume  $R=1.3A^{1/3}$ . Furthermore, the good fit obtained for  $L=0$  supports their contention that  $L=0$  transitions are more appropriately described by DWBA.

#### $F^{19}(d, \alpha_0)O^{17}$

For the transition to the ground state of  $O^{17}$ , the allowed values of  $L$  are 2 and 4. Using the same optical-model-potential parameters and cutoff-radius parameter as for the previous calculations, the differential cross sections for production of the ground state of  $O^{17}$  were calculated. The incoherent contributions were then determined using Eq. (3). The results are shown in Fig. 5.

The agreement with experiment is not as good as that obtained for production of the first excited state. Nevertheless, the theoretical curve does reproduce the general character of the experimental results. The relative proportions of the  $L=2$  and  $L=4$  components of the cross sections are consistent with those obtained by Takamatsu<sup>2</sup> and by Cosper *et al.*,<sup>3</sup> who used PWBA analyses for the same reaction at 14.7 and 9.2 MeV.

#### $F^{19}(d, \alpha_2)O^{17}$

This residual state has spin and parity  $\frac{1}{2}^-$ . There is no model which provides an adequate quantitative description of this state. Apart from the small cross sections, the angular distribution (Fig. 6) and energy dependence of the integrated cross sections (Fig. 9) have all the features of the data for the lower states of  $O^{17}$ . This would suggest that the mechanism for production of all three states is the same and that the smaller cross sections are a consequence of a small-structure factor. This can only be conjectured, however, because of the lack of a quantitative description of this  $\frac{1}{2}^-$  state.

The angular-momentum selection rules allow  $L=1$  for this state. The cutoff-radius DWBA calculation using the same optical-model-potential parameters, but with a slightly larger cutoff radius of 4.93 F, is shown in Fig. 6. Again the agreement with experiment is not spectacular, but the calculation does reproduce the general character of the angular distribution.

#### $N^{15}(d, \alpha)C^{13}$

The ground-state spin and parity of both  $N^{15}$  and  $C^{13}$  is  $\frac{1}{2}^-$ . In the shell-model description, this is attributed to the odd  $1p_{1/2}$  proton in  $N^{15}$  and to the odd  $1p_{1/2}$  neutron in  $C^{13}$ .<sup>45</sup> The first excited state of  $C^{13}$  has spin and parity  $\frac{1}{2}^+$ . Extensive measurements on the  $C^{12}(d, p)C^{13}$  reaction indicate that this is the  $2s_{1/2}$  shell-model state.<sup>25</sup> Although this would imply that the  $2s_{1/2}$  state lies lower in energy than the  $1d_{5/2}$  state, it has been shown that this inversion is possible through interaction of  $2s_{1/2}$  and  $1d_{5/2}$  nucleons with the  $1p_{1/2}$  shell.<sup>45</sup> Hence the  $(d, \alpha)$  reaction leading to this state by a pickup process should be inhibited, and this is indeed borne out by experiment (Fig. 7). The differential cross sections for production of this state are in general more than a factor of 2 smaller than those corresponding to the ground-state transitions. The fact that only a partial angular distribution was obtained precluded any detailed DWBA analysis.

The angular distribution for the  $N^{15}(d, \alpha_0)C^{13}$  reaction is shown in Fig. 8. These results are in agreement with those of Fischer and Fischer.<sup>15</sup> For the cutoff DWBA analysis for this reaction, the optical-model  $V$ ,  $W$ , and  $a$  parameters were the same as for the  $F^{19}(d, \alpha)O^{17}$  analysis. The radii of the incident deuteron and exit  $\alpha$ -particle channels were reduced to 3.80 and 4.26 F, respectively,

<sup>44</sup> Reference 35, p. 28.

<sup>45</sup> I. Talmi and I. Unna, *Ann. Rev. Nucl. Sci.* **10**, 353 (1960).

to account for the smaller radii of the  $N^{15}$  and  $C^{13}$  nuclei. Both  $L=0$  and  $L=2$  are allowed for this reaction. The best visual fit (Fig. 8) to these data was obtained for  $L=2$  with a cutoff radius of 3.30 F. This value is only slightly larger than the nuclear radius of  $N^{15}$ . This fit, though not striking, is substantially better than that obtained with  $L=0$ . An incoherent mixture of the  $L=0$  and  $L=2$  DWBA calculations gave no significant improvement to the fit. The DWBA fit is somewhat better than the PWBA fit obtained by Fischer and Fischer,<sup>15</sup> who also used  $L=2$ .

### CONCLUSIONS

The angular distributions for the  $(d, \alpha)$  reactions on  $F^{19}$  and  $N^{15}$  are fitted by the cutoff DWBA calculations.

The cutoff radii required for the fits were about 1 and 0.2 F larger than the target-nucleus radii for the  $F^{19}$  and  $N^{15}$  data, respectively. This is in fair agreement with the predictions of Buck and Rook<sup>36</sup> for cutoff-radius DWBA calculations. The best fit was obtained for the reaction  $F^{19}(d, \alpha_1)O^{17}$ , which proceeded primarily by  $L=0$  orbital-angular-momentum transfer. This result is also in accord with the speculations of Buck and Rook.<sup>36</sup> Although the theoretical calculations do not distinguish the reaction mechanism, i.e., pickup versus knockout, arguments based on the character of the nuclear states involved and the magnitudes of the experimental differential cross sections favor the pickup mechanism.

## Partial-Wave Analysis of Inelastic Electron Scattering on the Collective Giant Resonances of Medium and Heavy Spherical Even Nuclei\*

S. T. TUAN AND H. J. WEBER†  
Duke University, Durham, North Carolina

AND

L. E. WRIGHT  
Army Research Office, Durham, North Carolina and Duke University, Durham, North Carolina  
(Received 2 August 1967)

A partial-wave analysis of inelastic electron scattering on the giant (isospin) resonance is carried out for even medium and heavy spherical nuclei, taking into account the effects of finite energy loss. The giant resonance is treated collectively (Steinwedel-Jensen two-fluid model) by the dynamic coupling of the Goldhaber-Teller dipole mode to the collective quadrupole surface oscillations. The effects on the inelastic electron cross section due to the coupling of the surface phonons with their associated transition charge to the dipole modes are investigated. Since no experimental results are available yet, we calculate and discuss the electron scattering cross sections for several nuclei and compare them with the predictions of the pure dipole-mode model and the Born approximation. The nuclear parameters used are determined by fitting the photoabsorption cross section to experiment.

### I. INTRODUCTION

PREVIOUS work on the photoexcitation of the giant resonance of heavy deformed nuclei<sup>1</sup> indicated, firstly, that the structure of the giant resonance in the total photoabsorption cross section can be interpreted and understood as a collective dipole oscillation of a proton fluid against a neutron fluid (Steinwedel-Jensen two-fluid model)<sup>2</sup>; secondly, that the main structure results from the coupling of two collective modes, namely the dipole volume oscillations and the surface quadrupole vibrations of the nucleus (dynamic

collective model of Danos and Greiner). The situation in spherical medium and heavy nuclei is similar.<sup>3</sup> Because of the large energy ratio of the center of the dipole energy structure to the energy of the first excited  $2^+$  (collective, vibrational) state,  $\hbar\omega_1/\hbar\omega_2 \approx 20$ , the slow quadrupole oscillation does not change the nuclear surface appreciably during one dipole oscillation. Therefore, the giant resonance of a vibrating spherical nucleus essentially feels a deformed nuclear surface. The energy distribution of the dipole states is determined by the nuclear shape. Hence, we also have a strong dipole-quadrupole coupling for spherical nuclei through the boundary condition. This adiabaticity argument enables one to carry over to spherical

\* Supported in part by the U. S. Army Research Office (Durham) and the National Science Foundation.

† On leave from Frankfurt-am-Main University, Frankfurt, Germany.

<sup>1</sup> M. Danos and W. Greiner, Phys. Letters 8, 113 (1964); Phys. Rev. 134, B284 (1964); H. Arenhövel, M. Danos, and W. Greiner, Phys. Rev. (to be published).

<sup>2</sup> H. Steinwedel and J. H. D. Jensen, Z. Naturforsch. 5, 413 (1950).

<sup>3</sup> H. J. Weber, M. G. Huber, and W. Greiner, Z. Physik 190, 25 (1966); H. J. Weber, M. G. Huber, and W. Greiner, Z. Physik 192, 182 (1966); 192, 225 (1966); M. G. Huber, M. Danos, H. J. Weber, and W. Greiner, Phys. Rev. Letters 15, 529 (1965); Phys. Rev. 155, 1073 (1967); H. Arenhövel and H. J. Weber, Nucl. Phys. A91, 145 (1967).